Taylor & Francis
Taylor & Francis Group

Inhalation Toxicology

International Forum for Respiratory Research

ISSN: 0895-8378 (Print) 1091-7691 (Online) Journal homepage: https://www.tandfonline.com/loi/iiht20

The Biopersistence of Brazilian Chrysotile Asbestos Following Inhalation

David M. Bernstein, Rick Rogers & Paul Smith

To cite this article: David M. Bernstein, Rick Rogers & Paul Smith (2004) The Biopersistence of Brazilian Chrysotile Asbestos Following Inhalation, Inhalation Toxicology, 16:11-12, 745-761, DOI: 10.1080/08958370490490176

To link to this article: https://doi.org/10.1080/08958370490490176

Inhalation Toxicology, 16:745–761, 2004

ISSN: 0895-8378 print / 1091-7691 online
DOI: 10.1080/08958370490490176

Taylor & Francis
healthsciences

The Biopersistence of Brazilian Chrysotile Asbestos Following Inhalation

David M. Bernstein
Consultant in Toxicology, Geneva, Switzerland

Rick Rogers
Rogers Imaging Corporation, Needham, Massachusetts, USA

Paul Smith
Research & Consulting Company Ltd., Füllinsdorf, Switzerland

With the initial understanding of the relationship of asbestos to disease, little information was available on whether the two different groups of minerals that are called asbestos were of similar or different potency in causing disease. Asbestos was often described as a durable fiber that if inhaled would remain in the lung and cause disease. It has been only more recently, with the development of a standardized protocol for evaluating the biopersistence of mineral fibers in the lung, that the clearance kinetics of the serpentine chrysotile have been shown to be dramatically different from those of amphibole asbestos, with chrysotile clearing rapidly from the lung. In addition, recent epidemiology studies also differentiate chrysotile from amphibole asbestos. The biopersistence studies mentioned have indicated that chrysotile from Canada and California clear rapidly from the lung once inhaled. However, variations in chrysotile mineralogy have been reported depending upon the region. This is most likely associated with variations in the forces which created the chrysotile fibers centuries ago. In the present study, the dynamics and rate of clearance of chrysotile from the Cana Brava mine in central Brazil was evaluated in a comparable inhalation biopersistence study in the rat. For synthetic vitreous fibers, the biopersistence of the fibers longer than 20 μm has been found to be directly related to their potential to cause disease. This study was designed to determine lung clearance (biopersistence) and translocation and distribution within the lung. As the long fibers have been shown to have the greatest potential for pathogenicity, the chrysotile samples were specifically chosen to have more than 450 fibers/cm^3 longer than 20 μm in length present in the exposure aerosol. For the fiber clearance study (lung digestions), at 1 day, 2 days, 7 days, 2 wk, 1 mo, 3 mo, 6 mo, and 12 mo following a 5-day (6 h/day) inhalation exposure, the lungs from groups of animals were digested by low-temperature plasma ashing and subsequently analyzed by transmission electron microscopy (at the GSA Corp.) for total chrysotile fiber number in the lungs and chrysotile fiber size (length and diameter) distribution in the lungs. This lung digestion procedure digests the entire lung with no possibility of identifying where in the lung the fibers are located. A fiber distribution study (with confocal microscopy) was included in order to identify where in the lung the fibers were located. At 2 days, 2 wk, 3 mo, 6 mo, and 12 mo postexposure, the lungs from groups of animals were analyzed by confocal microscopy to determine the anatomic fate, orientation, and distribution of the retained chrysotile fibrils deposited on airways and those fibers translocated to the broncho-associated lymphoid tissue (BALT) subjacent to bronchioles in rat lungs. While the translocation of fibers to the BALT and lymphatic tissue is considered important as in cases of human's with asbestos-related disease, there has been no report in the literature of pathological changes in the BALT and lymphatic tissue stemming from asbestos. Thus, if the fibers are removed to these tissues, they are effectively neutralized in the lung.

Received 12 May 2004; accepted 27 May 2004.
This study was sponsored by a grant from SAMA Mineraçào de Amianto LTDA.
Address correspondence to Dr. David M. Bernstein, Consultant in Toxicology, 40 chemin de la Petite-Boissière, 1208 Geneva, Switzerland. E-mail: davidb@itox.ch

Chrysotile was found to be rapidly removed from the lung. Fibers longer than 20 μm were cleared with a half-time of 1.3 days, most likely by dissolution and breakage into shorter fibers. Shorter fibers were also rapidly cleared from the lung with fibers 5–20 μm clearing even more rapidly ($T_{1/2} = 2.4$ days) than those $<5\mu$m in length ($T_{1/2\,\text{weighted}} = 23$ days). Breaking of the longer fibers would be expected to increase the short fiber pool and therefore could account for this difference in clearance rates. The short fibers were never found clumped together but appeared as separate, fine fibrils, occasionally unwound at one end. Short free fibers appeared in the corners of alveolar septa, and fibers or their fragments were found within alveolar macrophages. The same was true of fibers in lymphatics, as they appeared free or within phagocytic lymphocytes. These results support the evidence presented by McDonald and McDonald (1997) that the chrysotile fibers are rapidly cleared from the lung in marked contrast to amphibole fibers which persist.

With the initial understanding of the relationship of asbestos to disease, little information was available on whether the two different minerals that are called asbestos were of similar or different potency in causing disease. Asbestos was often described as a durable fiber that if inhaled would remain in the lung and cause disease. It has been only more recently with the development of a standardized protocol for evaluating the biopersistence of mineral fibers in the lung (Bernstein & Riego-Sintes, 1999) that the clearance kinetics of the serpentine chrysotile have been shown to be dramatically different from those of amphibole asbestos with chrysotile clearing rapidly from the lung (Bernstein et al., 2003a, 2003b). In addition, recent epidemiology studies also differentiate chrysotile from amphibole asbestos (Hodgson & Darnton, 2000; Berman & Crump, 2004).

The biopersistence studies mentioned have indicated that chrysotile from Canada and California clear rapidly from the lung once inhaled. However, variations in chrysotile mineralogy have been reported depending upon the region. This is most likely associated with variations in the forces which created the chrysotile fibers centuries ago. In the present study, the dynamics and rate of clearance of chrysotile from the Cana Brava mine in central Brazil was evaluated in a comparable inhalation biopersistence study in the rat.

As with the other biopersistence studies of chrysotile, the protocol for this study was designed to meet the specific recommendations of the European Commission (EC) Interim Protocol for the Inhalation Biopersistence of synthetic vitreous fibers (Bernstein & Riego-Sintes, 1999). For synthetic vitreous fibers, the biopersistence of the fibers longer than 20 μm has been found to be related to their potential to cause disease (Bernstein, 1998; Bernstein et al., 2001a, 2001b). As is described later, the specifications in the protocol for counting and sizing the fibers were modified to accommodate the finer dimensions of the chrysotile fibers in comparison to mineral fibers. In addition, the disposition of fibers within the lung was also determined using confocal microscopy.

METHODS

The exposure and in-life phases of the study were performed at the Research and Consulting Company Ltd., Füllinsdorf, Switzerland. Fiber counting and sizing were performed under subcontract to RCC at Gesellschaft für Staubmesstechnik und Arbeitsschutz GmbH (GSA), Neuss, Germany. The confocal microscopy analysis was performed by Rogers Imaging Corporation, Needham, MA.

Chrysotile Sample Characteristics

The chrysotile fibers used in this study were obtained from the Cana Brava Mine located in Minasu in the state of Goias in Brazil. The chrysotile fiber is monoclinic in crystalline structure and has a unique rolled structure described below. The fibers are present in the mine in all length categories ranging from "long" (greater than 10 mm: grades 4T, 4K, 4A, and 3T on the Canadian Quebec Screening Scale [QSS]; Cossette & Delvaux, 1979), to medium (fibers between 5 and 9 mm: QSS grades 4X, 4Z, and 5K), to "short" (below 5 mm: QSS grades 5R, 6D, 7M, and 7T).

The chemical composition and the structure of chrysotile are markedly different from that of amphiboles such as tremolite or amosite (Hodgson, 1979), as shown in Table 1. The chemistry of chrysotile is composed of a silicate sheet of composition $(Si_2O_5)_n^{2n-}$, in which three of the O atoms in each tetrahedron are shared with adjacent tetrahedral and a nonsilicate sheet of composition $[Mg_3O_2(OH)_4]_n^{2n+}$. In chrysotile the distances between apical oxygens in a regular (idealized) silicate layer are shorter (0.305 nm) than the O–O distances in the ideal Mg-containing layer (0.342 nm), which may account for the curling of the layers, which results in the rolling up like a carpet to form concentric hollow cylinders (Skinner et al., 1988). This structure is illustrated in Figure 1a (Speil & Leineweber, 1969), and transmission electron micrographs of the Cana Brava chrysotile are shown in Figure 1b. The Mg molecule is on the outside of the curl and is thus exposed to the surrounding environment.

In contrast, with amphiboles such as tremolite, the basic structure is in the form of an I-beam with corner-linked $(SiO_4)^{4-}$ tetrahedral linked together in a double-tetrahedral chain that sandwiches a layer with the Ca_2Mg_5. In contrast to chrysotile, with tremolite, the Mg is locked within the I-beam structure. This is illustrated in Figure 2.

TABLE 1
Typical chemical composition (percent)

Compound	Chrysotile[a]	Tremolite[b]	Amosite[b]
SiO_2	40.90	55.10	49.70
Al_2O_3	5.88	1.14	0.40
Fe_2O_3	6.85	0.32	0.03
FeO	—	2.00	39.70
MnO	—	0.10	0.22
MgO	34.00	25.65	6.44
CaO	Trace	11.45	1.04
K_2O	0.02	0.29	0.63
Na_2O	0.03	0.14	0.09
H_2O^+	[c]	3.52	1.83
H_2	[c]	0.16	0.09
CO_2	[c]	0.06	0.09
Ignition loss[c]	12.20		
Total	99.95	99.93	100.26

[a]Cana Brava Mine.
[b]Hodgson (1979), pp. 80–81.
[c]H_2O^+, H_2, and CO_2 are included together as ignition loss in the analysis.

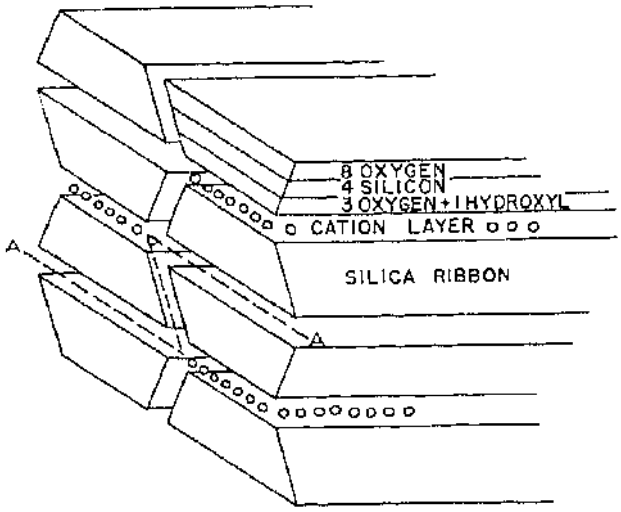

FIG. 2. Schematic representation of the chemical structure of amphiboles showing the cation layer which is locked within the I-beam structure (reproduced from Speil and Leineweber (1969), Figure 9, p. 174).

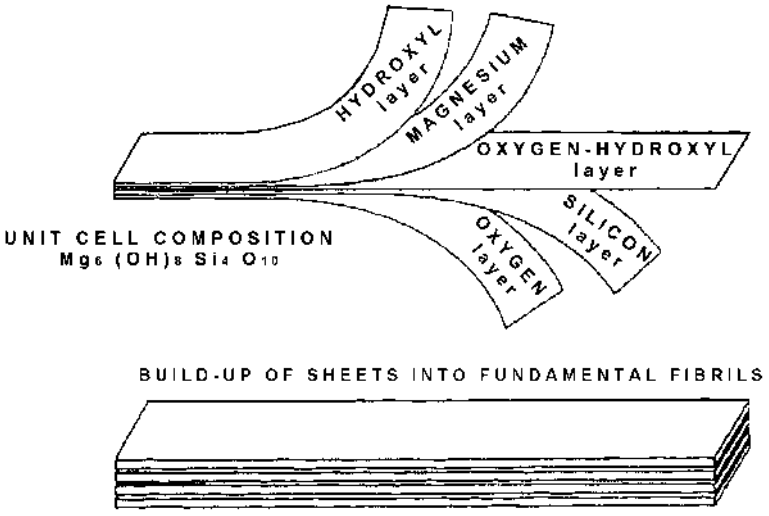

(a)

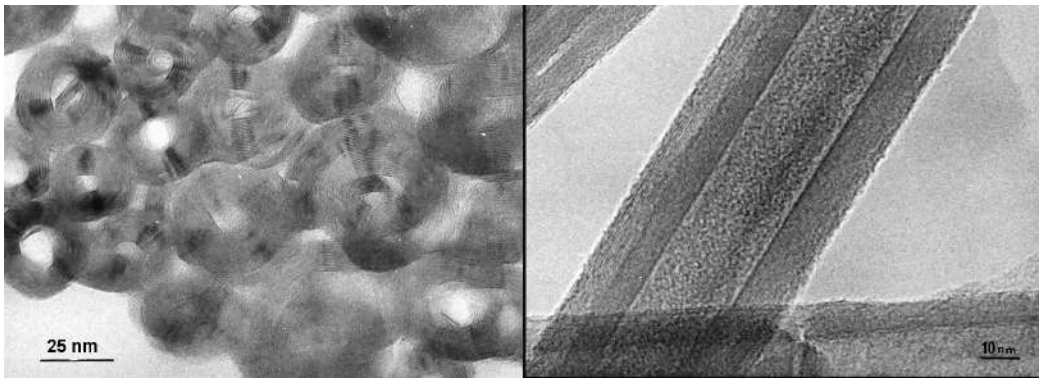

(b)

FIG. 1. (a) Illustration of the layered structure of chrysotile. From Speil & Leineweber (1969). (b) Transmission electron micrographs of chrysotile showing the coiled sheet like form of the fibers (Cruxên Barros de Oliveira, 1989).

TABLE 2
Summary results from aerosol generation trials

	CA 600	CA 500	CA 400	CA 300
First aerosol generation				
Achieved concentration (mg/m^3)	6.3	12.6	6.9	9.0
Second aerosol generation				
Achieved concentration (mg/m^3)	Not performed	2.2	9.0	8.3
Number of total fibers/cm^3	12,968	8743	23,435	28,990
Number of WHO fibers/cm^3	2977	1935	5364	7648
Number of WHO fiber longer than 20 μm/cm^3	595	358	1875	3132
Percentage of WHO fibers/total fibers	23%	22%	23%	26%
Percentage long fibers/total fibers	5%	4%	8%	11%
Percentage long fibers/WHO fibers	20%	19%	35%	41%

Chrysotile Selection

Prior to the start of exposure, an aerosol generation trial (RCC project 634048) was performed on samples from four commercial chrysotile grades, one from each primary production grade produced. The purpose of this trial was to choose the chrysotile fiber grade with the largest fraction of fibers longer than 20 μm in length and to assure that the sample could be aerosolized uniformly without degradation in size distribution. The results from these trials are shown in Table 2. The CA300 grade was chosen for the biopersistence study as it best met the stated criteria.

Experimental Design

The experimental design of the in-life and biopersistence analysis has been presented in detail previously (Bernstein et al., 1994, 2003a, 2003b) and is summarized here. In particular, details of the counting and sizing procedures are reiterated as these are considered essential to the successful interpretation of these studies.

Animal exposure. Groups of 56 (4–8 wk old) male Fischer 344 rats (SPF quality) were exposed by flow-past nose-only exposure to a target fiber aerosol concentration of 450 fibers L > 20 μm/cm^3 for 6 h/day for a period of 5 consecutive days. This concentration corresponded to three times that required by the EC Biopersistence Protocol (Bernstein & Riego-Sintes, 1999) in order to assure that there is no question of sufficient long fiber exposure and is the highest concentration of long fibers ever reported used in a rodent inhalation study. In addition, a negative control group was exposed in a similar fashion to filtered air. To be comparable with current and previous fiber inhalation studies, Fischer 344 rats [CDF (F-344)/CrlBR] obtained from Charles River Laboratories (Kingston, NY) were used.

Exposure system. The fiber aerosol generation system was designed to loft the bulk fibers without breaking, grinding or contaminating the fibers (Bernstein et al., 1994). The animals were exposed by the flow-past nose/snout-only inhalation exposure system. This system was derived from Cannon et al. (1983) and is different from conventional nose-only exposure systems in that fresh fiber aerosol is supplied to each animal individually and exhaled air is immediately exhausted.

Fiber clearance. At 1 day, 2 days, 7 days, 2 wks, 1 mo, 3 mo, 6 mo, and 12 mo postexposure, the lungs from groups of animals were digested by low-temperature plasma ashing and subsequently analyzed by transmission electron microscopy (at the GSA Corp.) for total chrysotile fiber number in the lungs and chrysotile fiber size (length and diameter) distribution in the lungs. This lung digestions procedure digests the entire lung with no possibility of identifying where in the lung the fibers are located.

Fiber distribution. This procedure was undertaken to determine the distribution of fibers within various pulmonary compartments. At 2 days, 2 weeks, 3 mo, 6 mo, and 12 mo postexposure, the lungs from groups of animals were prepared and analyzed by confocal microscopy. The locations of chrysotile fibrils deposited on airways as well as those fibers translocated to the broncho-associated lymphoid tissue (BALT) subjacent to bronchioles were studied.

Lung Digestion for Fiber/Particle Analysis

From 7 rats per group per time point in the CA300 exposure group and 7 rats per group at 1 day, 1 mo, 6 mo, and 12 mo in the air control exposure group the lungs were thawed and the entire lung was prepared for analysis. The tissue was initially dehydrated by freeze drying (Edwards EF4 Modulyo freeze dryer) and dried to constant weight to determine the dry weight of the tissue. The dry tissue was plasma ashed in an LFE LTA 504 multiple chamber plasma unit at 300 W for at least 16 h. Upon removal from the ashing unit, the ash from each lung was weighed and suspended in 10 ml methanol using a low-intensity ultrasonic bath. The suspension was then transferred into a glass bottle with the combustion boat rinse and the volume was made up to 20 ml. An aliquot was then removed and filtered onto a gold-coated polycarbonate filter (pore size of 0.2 μm).

Validation

The analytical procedures used for fiber recovery (lung digestion and transmission electron microscopy) have been validated using an independent comparative analysis with confocal microscopy, which is noninvasive (a cube of the lung was analyzed in three dimensions), and have been shown not to bias the size distribution or number of the measured fibers.

Counting Rules for the Evaluation of Air and Lung Samples by Transmission Electron Microscopy

All fibers visible at a magnification of 10,000× were taken into consideration. All objects seen at this magnification were sized with no lower or upper limit imposed on either length or diameter. The bivariate length and diameter was recorded individually for each object measured. Fibers were defined as any object that had an aspect ratio of at least 3:1. The diameter was determined at the greatest width of the object. All other objects were considered as nonfibrous particles.

The stopping rules for counting of each sample were defined as follows: For nonfibrous particles, the recording of particles was stopped when a total of 30 particles were recorded. For fibers, the recording was stopped when 500 fibers with length ≥ 5 μm, diameter ≤ 3 μm (WHO, 1985), or a total of 1000 fibers and nonfibrous particles were recorded. If this number of fibers was not reached after evaluation of 0.15 mm^2 of filter surface, additional fields of view were counted until either 500 WHO fibers was reached or a total of 5 mm^2 of filter surface was evaluated, even if a total of 500 countable WHO fibres was not reached. The evaluation of short fibers (length <5 μm) was stopped when 100 short fibers was reached.

Confocal Imaging of Fibers and Lung Tissue

The lungs of animals designated for confocal microscopy analysis were fixed in Karnovski's fixative by gentle instillation under a pressure of 30 cm H_2O for 2 h with simultaneous immersion in fixative. The trachea was then ligated and the inflated lungs were stored in the same fixative. Following fixation, apical lobes were divided into five pieces ($10\ mm^2 \times 5$ mm thick), cut parallel to the hilum, dehydrated in graded ethanolic series to absolute, stained with 0.005% lucifer yellow, and embedded in Spurr plastic for microscopic analysis (Rogers et al., 1999). Flat surfaces were prepared from hardened plastic blocks containing embedded lung pieces by glass knife microtomy. The apical lobe was chosen as deposition measurements in small laboratory rodents (Raabe et al., 1977) showed higher deposition in the right apical lobe.

Simultaneous fiber and lung imaging. To determine the anatomic orientation and distribution of the retained chrysotile fibrils in lung tissue, large areas of lung were examined en bloc. A Sarastro 2000 CLSM fitted with a 25-mW argon-ion laser configured for fluorescent and reflected light imaging was used to obtain micrographs. Images were recorded using light reflected (488 nm excitation, <510 nm emission) from fibers using 40× or 60× planApo objectives. Increased sensitivity of the reflected light signal was achieved by use of a 488-nm notch filter in front of the PMT used to detect images of fibers. Fluorescent emission spectra >510 nm were directed to a separate detector to image cellular morphology and lung structure. Digital images were superimposed to show fiber positions in relation to lung tissue where image 1 of the pair contained lung structures (gray) and airspace (black), and image 2 of the pair revealed fibers (red). Selected airways and lung compartments containing fibers were scanned and three-dimensional projections generated from serial optical sections of lung to reveal fiber orientation and distribution of fibers in lung tissue. Three-dimensional projections were generated using ImageSpace or Voxel View software (Vital Images, Inc., Fairfield, IA). To improve visual presentation of the reconstructed data, fiber profiles were subjected to a segmentation procedure to remove spectral cross talk between the serial section stack containing lung and the serial section stack of images containing fibers.

Image analysis. Digital micrographs were composed of a matrix (x,y) array of pixels, each with an intensity value from 0 to 255 gray-scale units. Optical sections in the z-axis were recorded by adjusting the stage height using stepper motors. Pixel intensity values of fluorescent-labeled lung tissue was measured directly from images and expressed quantitatively using threshold techniques. Two-dimensional object counting procedures and three-dimensional digital planimetry (ImageSpace, Molecular Dynamics) were used to count fibers. Pixel intensities unique to the lungs, fibers, and airspaces in the paired micrographs were summed to give area measurements. To obtain volumetric information, optical section thickness was determined using the full-width half-maximum procedure (Brismar et al., 1996) and multiplied by tissue area. Precise morphometric data such as quantification of fluorescence intensity, point-to-point distances, number of occurrences per field, surface versus bound structures, area, and volume measurements were obtained directly from images in this manner.

Confocal Fiber Quantification

Fiber distribution. Two to five pieces of lung tissue from the right apical lobe were examined from each animal. Fields of view containing lymphatic tissue profiles were selected from each piece and images were recorded. Fiber profiles in each micrograph were counted and expressed as the number of fibers per area of lung tissue identified by compartment. For the purposes of this study, lung tissue was divided into several compartments. Airway profiles with lumenal diameters less than 300 μm were included in the airway compartment. Fields of lung showing alveolar septa and/or alveolar duct profiles were included in the alveolar compartment. Lymphatic compartment was identified separately from interstitium.

In situ microscopic analysis. Two types of analysis were performed: one to determine the number of fibers per lung and their average lengths, and another to identify the distribution of fibers among lymphatic verses nonlymphatic compartments. To determine the number of fibers per lung, fibers were counted from confocal micrographs recorded from three to five regions of each apical lung lobe. Tissue area and numbers of fibers per micrograph were then converted to fibers per tissue volume by multiplying by the section thickness. Lung volumes were estimated by stereologic point counting (Weibel, 1984) or digital planimetry (ImageSpace software, Molecular Dynamics, Sunnyvale, CA). In order to determine the numbers of fibers per lung, fiber length was determined from serial section analysis. Based on the average fiber lengths, the numbers of fibers were then estimated from these volumes. Since the lung fiber per lung measurement is very sensitive to fiber position relative to the plane of focus, the number of fiber profiles were counted and multiplied by the average fiber length measured en bloc from serial section analysis techniques. From these calculations, the per lung number of fibers (<5 μm, 5–20 μm, and >20 μm) were determined for each of the exposure groups.

Fiber dimensions. Fiber lengths measured from aerosolized fibers prior to exposure and post inhalation (left lung) were determined by TEM analysis and compared to in situ fiber lengths in lungs as measured from microscopic serial optical sections. To accurately measure fiber lengths in situ, the optical section thickness was calculated for each objective used. Optical section thickness was 1.5 μm for images recorded from a 40× (1.0 NA) oil immersion objective, and 1.3 μm thick for sections recorded from a 60× PlanApo (1.4 NA) oil immersion objective. Fiber orientation relative to optical sections was adjusted to the total distance traversed by the stepper motor during the sectioning process.

RESULTS

Inhalation Biopersistence

The EC Inhalation Biopersistence Protocol specifies that the exposure atmosphere to which the animals are exposed should have at least 100 fibers/cm^3 longer than 20 μm. In this study, the number of fibers longer than 20 μm in the exposure atmosphere was purposely increased to a mean of 465 fibers with L > 20 μm/cm^3, in order to maximise any potential effect of these long fibers on clearance from the lung. The number concentration and size distribution of the air control and chrysotile exposure group are shown in Table 3. These results differ from the pretrial selection results from Table 2, as the final CA300 sample used in the study was taken from a different commercial batch.

As illustrated in Figure 3, all of the longer fibers (L > 20 μm) in the exposure atmosphere were less than 0.6 μm in diameter and thus potentially respirable. Figure 4 shows the bivariate length and diameter distribution of the fibers recovered from the lung at 1 day following cessation of exposure. The mean fiber concentrations and dimensions are presented in Table 4 for all eight time points.

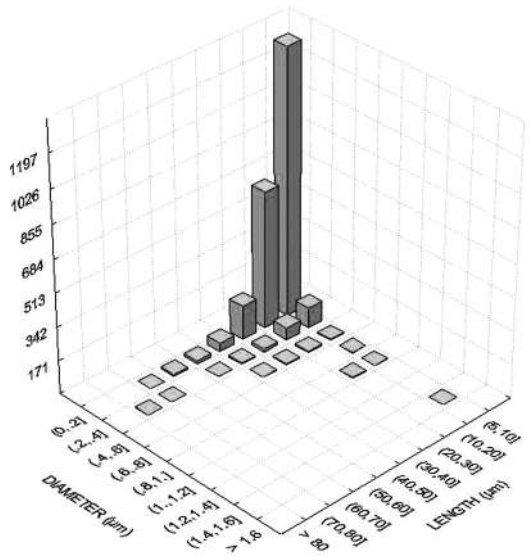

FIG. 3. Chrysotile fibers in the exposure atmosphere, bivariate (length and diameter) histogram of WHO fibers.

Fiber Clearance

The fibers longer than 20 μm that deposit in the lung rapidly "disappear" from the lung as shown in Figure 5 with a clearance half-time of the fibers longer than 20 μm of 1.3 days. The clearance half-times (Table 5) were determined using the procedures specified in the EC Inhalation Biopersistence protocol.

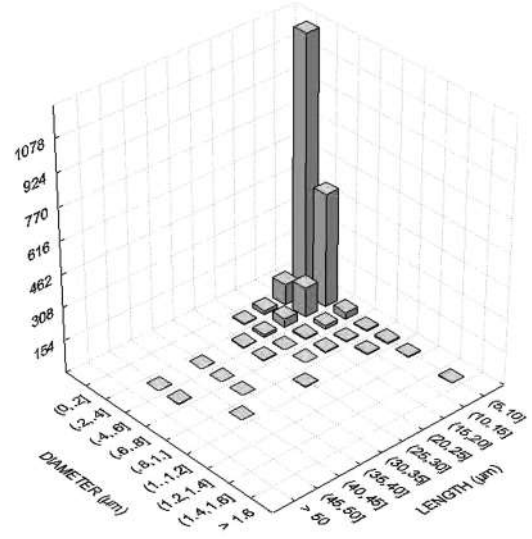

FIG. 4. Chrysotile fibers in the lung at 1 day following cessation of exposure, bivariate (length and diameter) histogram of WHO fibers.

TABLE 3

Number and size distribution of the fibers in the chrysotile exposure aerosol

Exposure group	Gravimetric concentration (mg/m^3)	Number of fibers evaluated	Number of total fibers/cm^3	WHO fibers/ cm^3	Percent WHO fibers	Number of fibers $\geq$20 μm/cm^3	Percent of WHO fibers $\geq$20 μm/cm^3	Diameter range (μm)	Length range (μm)	GMD (μm) (SD)	GML (μm) (SD)	Mean diameter (SD)	Mean length (SD)	Length weighted arithm. diameter (μm)	Length weighted geom. diameter (μm)	Aspect ratio
Air control	$-0.07^{(a)}$ (0.03)	15	0	0	—	0	—	0.03–0.4	0.9–4.5	0.13 (2.15)	1.73 (1.49)	0.17 (0.10)	1.88 (0.086)	0.18	0.16	17.3
Chrysotile CA 300	4.32 (0.36)	3079	9226	2098	23%	465	22%	0.01–1.5	0.6–80	0.12 (1.93)	2.75 (2.36)	0.15 (0.09)	4.33 (5.85)	0.14	0.11	52.0

[a]Negative values are attributed to filter weight variations due to the dehumidification in the dry air used during exposure. This value is presented here as an indication of the degree of accuracy of the weighing method.

TABLE 4
Mean fiber concentrations and dimensions of the fibers recovered from the lungs at each time point

	Sacrifice time point (time since cessation of last exposure)							
	1 day	2 days	7 days	2 weeks	1 mo	3 mo	6 mo	12 mo
Determined following lung digestion using transmission electron microscopy								
Number fibers evaluated	4046	4033	1290	1147	841	673	751	868
Total number of fibers/lung $\times 10^6 \pm$ SD	38.2 ± 15.2	28.8 ± 5.5	10.3 ± 3.5	10.8 ± 4.5	6.3 ± 2.3	3.0 ± 0.5	4.2 ± 0.5	1.1 ± 0.1
WHO Fibers/lung $\times 10^6 \pm$ SD	5.5 ± 1.2	5.0 ± 0.6	0.7 ± 0.2	0.6 ± 0.1	0.3 ± 0.08	0.2 ± 0.03	0.2 ± 0.03	0.3 ± 0.03
Percent of Total	14.4%	17.5%	6.8%	5.3%	4.8%	5.1%	5.3%	29.3%
Number fibers L $\geq 20\mu$ m/lung $\times 10^6 \pm$ SD	0.148 ± 0.248	0.114 ± 0.310	0.006 ± 0.002	0.002 ± 0.002	0.002 ± 0.002	0.000	0.001 ± 0.002	0.014 ± 0.006
Percent of Total	0.4%	0.4%	0.1%	0.0%	0.0%	0.0%	0.0%	1.2%
Number fibers L $< 5\mu$m/lung $\times 10^6 \pm$ SD	32.7 ± 14.1	23.8 ± 5.2	9.6 ± 3.5	10.2 ± 4.4	6.0 ± 2.2	2.9 ± 0.5	4.0 ± 0.5	0.8 ± 0.1
Percent of total	85.6%	82.5%	93.2%	94.7%	95.2%	94.9%	94.7%	70.7%
Diameter range (μm)	0.03–1.5	0.03–2.0	0.01–0.8	0.01–0.8	0.03–2.0	0.03–0.7	0.03–0.8	0.02–0.7
Length range (μm)	0.3–50	0.4–60	0.5–25	0.5–20	0.7–20	0.7–18	0.5–20	0.7–35
GMD (μm)	0.11	0.13	0.11	0.11	0.13	0.12	0.11	0.11
SD	2.01	1.88	1.89	1.85	1.76	1.89	1.69	2.01
GML (μm)	2.32	2.58	1.87	1.86	1.79	1.79	1.97	3.63
SD	1.98	1.94	1.80	1.71	1.69	1.69	1.69	1.84
Mean diameter (μm)	0.14	0.16	0.13	0.13	0.15	0.14	0.12	0.14
SD	0.11	0.09	0.07	0.07	0.08	0.08	0.06	0.09
Mean length (μm)	3.01	3.27	2.26	2.19	2.08	2.10	2.30	4.42
SD	2.78	2.78	1.71	1.51	1.41	1.46	1.52	3.35
Length weighted geometric diameter (μm)	0.15	0.15	0.12	0.12	0.14	0.13	0.12	0.12
Aspect ratio	26.9	26.9	25.5	23.7	18.2	20.8	23.5	44.3
Determined by confocal microscopy								
Mean length, μm (SD)	—	5.12 (2.94)	—	5.72 (3.79)	—	4.22 (2.35)	4.89 (2.24)	3.91 (1.93)

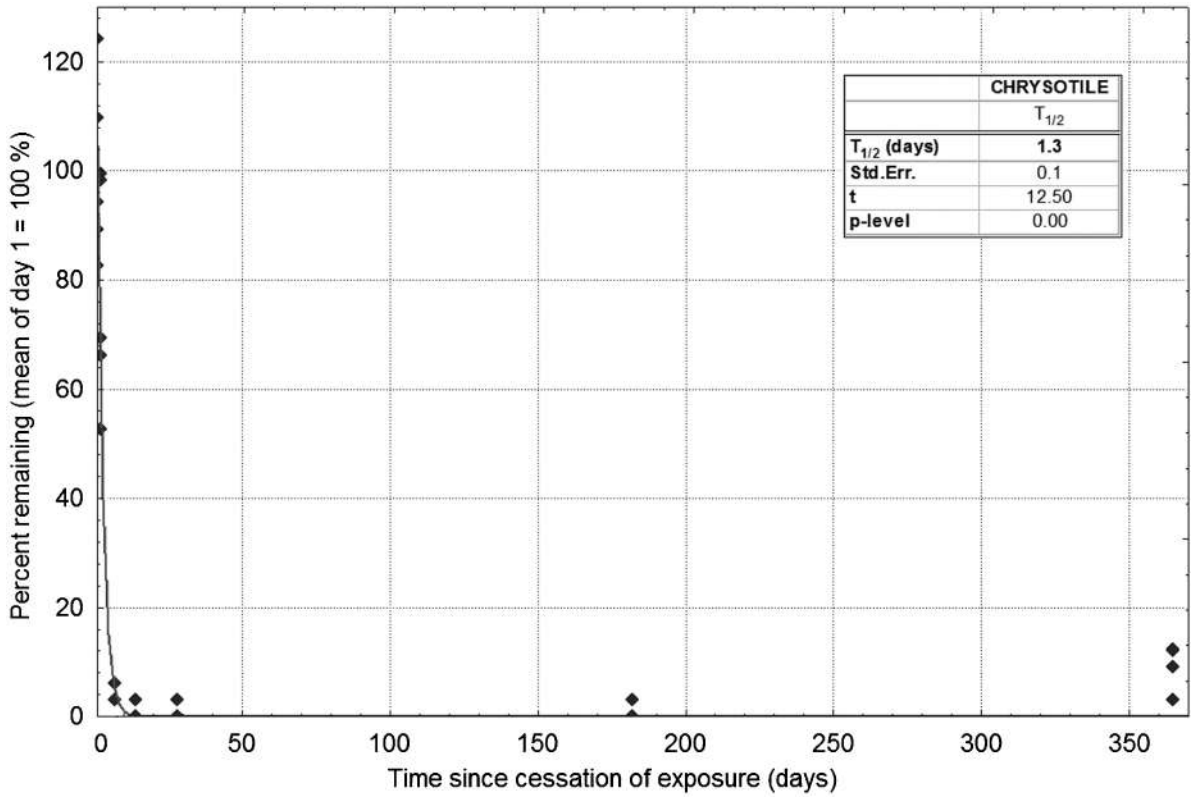

FIG. 5. Biopersistence of chrysotile fibers L > 20 μm.

No fibers longer than 20 μm were observed at 91 days post-exposure. At 182 days, 1 long fiber was found in 1 rat, and at 365 days, 1, 3, or 4 long fibers were found out of a total of 250 fibers evaluated in these samples on the aliquot filter. This number of fibers when extrapolated to the whole lung corresponds to 900 fibers L > 20 μm/lung at 182 days and 13,500 fibers L > 20 μm/lung at 365 days. After similar exposure of the insoluble amphibole fiber amosite, there would be approximately 2,000,000 fibers L > 20 μm/lung remaining at 182 days and 1,300,000 fibers L > 20 μm/lung remaining at 365 days (extrapolated from Hesterberg et al., 1998a).

As seen in Table 4, all length fractions clear rapidly from the lung. By 6 mo following cessation of exposure, the percent of WHO fibers in the total appears to stabilise around 5%. However, at 12 mo it increases to 29% which could suggest that the shorter fibers less than 5 μm in length are dissolving or clearing more rapidly. While the mean diameter does not change significantly, suggesting that the fibers are breaking apart, the upper range of diameters does decrease.

TABLE 5
Clearance half-times of Brazilian chrysotile for each length fraction

Fiber length	Clearance half-time $T_{1/2}$
> 20 μm	1.3 days
WHO/5–20 μm	2.4 days
<5 μm	Weighted $T_{1/2}$ 23 days, 2.5 fast phase/133 slow phase

Confocal Microscopic Analysis

The classic biopersistence study as defined by the EC protocols involves the digestion of the entire rat lung for the determination of the fiber number and size distribution at each time point. The TEM analysis of ashed samples provides a measure of only the total number and size of fibers that are removed from the lung. It cannot detect where the fibers are located within the lung.

In order to determine the disposition of those fibers remaining in the lung, confocal microscopic analysis was performed on lobes of lungs embedded in plastic. A lens such as the one on a microscope that is closest to the sample to be examined (the objective lens) brings light to a focus at a certain fixed distance. If the lens is well designed and constructed, there will be a plane where objects will be in focus. To use a conventional microscope effectively, it is necessary to cut a very thin slice of material to avoid tissue above and below the plane of focus from degrading the quality of the final image. The confocal microscope goes beyond the conventional microscope in this regard, because it excludes out-of-focus light, using a light-limiting

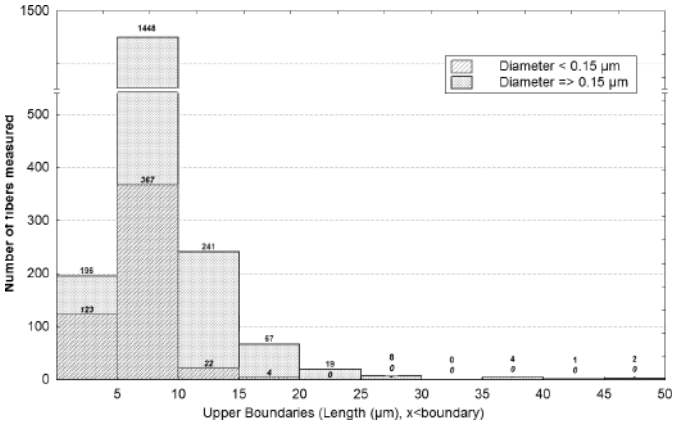

FIG. 6. Length, $d < 0.15$ μm and $d \geq 0.15$ μm at 1 day, from lung digestion procedure using transmission electron microscopy.

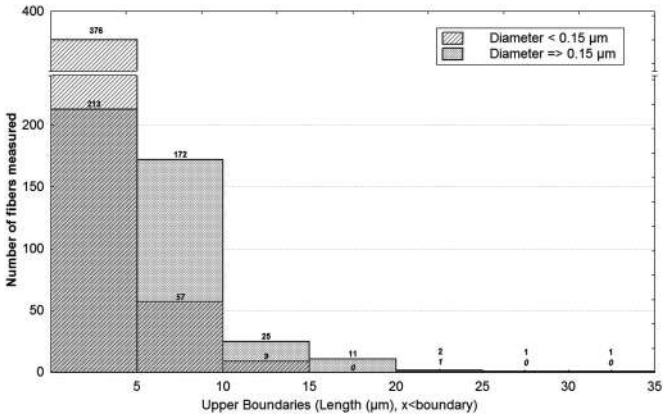

FIG. 7. Length, $d < 0.15$ μm and $d \geq 0.15$ μm at 1 yr, from lung digestion procedure using transmission electron microscopy.

aperture to form a sharp, high-quality image even if there is material present that is not at the plane of focus. This means that specimens do not have to be thin sectioned before they can be examined. Instead, it is possible to obtain an image of the material at the plane of focus even if that plane lies several hundred micrometers deep within the specimen.

Microscopic appearance of the chrysotile fibers retained in lung. The limit of detection of the confocal method used to quantify the disposition of the chrysotile fibers in the lung was approximately 150 nm point-to-point resolution. Since most fibers were oriented to present various oblique profiles in longitudinal orientation, most fibrils greater than 150 nm in diameter were detected. This provided an accurate account of all fibers longer than 20 μm in the lung on day 1 as shown in Figure 6, as all such fibers observed by TEM were thicker than 0.15 μm. Shorter fibers with diameters greater than 0.15 μm were present in considerably larger number than thinner fibers (diameter <0.15 μm) such as to provide an excellent account of the disposition of these length fibers as well. Similar results were seen throughout the study with the results from 12 mo shown in Figure 7. It is interesting to note that the shorter, thinner fibers (especially below 5 μm in length) are increasing in percentage, which suggests that the remaining chrysotile continues to dissolve in the lung.

Unfortunately, no confocal examination was planned on day 1 following cessation of exposure as the clearance was not expected to be so rapid. The first time point observed using the confocal microscopy was on day 2 following cessation of the 5-day exposure.

At 2 days, the chrysotile fibers appeared to have been well distributed throughout the lung in both airway and parenchyma. Fibers appeared as separate, fine fibrils, occasionally unwound at one end and were not found clumped together. Fibers were found on the ciliated airways and in airway macrophages (Figure 8, c, f), alveoli and in lymphatic ducts (Figure 8, b, e). An occasional long fiber was found in alveoli (Figure 8, a, d) with other shorter fibers partially phagocytized by alveolar macrophages. As the exposure was 5 days in duration, at 2 days following the last exposure the fibers had between 2 and 6 days to clear. With a clearance time of 1.3 days, few long fibers would remain even at 2 days.

At 2 wk following cessation of exposure, chrysotile fibers are clearly observed on the ciliated airways, indicating that the ciliated mucous transport of fibers is still active (Figure 9, c, f). Alveolar macrophages are observed phagocytizing chrysotile fibers, although the length of fibers observed is considerably shorter than that observed at 2 days post exposure (Figure 9, a, d). Fibers are also observed in the distal lymphatics (Figure 9, b, e), both free and in phagocytic lymphocytes.

At 3 mo postexposure, there is even a further notable reduction in the number and in the length of fibers observed. Macrophages are still occasionally observed in the alveoli phagocytising small chrysotile fibers and nonfibrous fragments (Figure 10, a, d). These short fibers and nonfibrous fragments are also observed on the alveolar epithelium. (Figure 10, b, e). By 6 mo postexposure, primarily shorter fibers are observed either on the epithelial or alveolar surface (Figure 10, c, f) or in the lymphatics. The fibers within the alveoli are not associated with alveolar macrophages.

The numbers of fibers observed as a function of time in the airspace, bronchial and alveolar epithelium, interstitium, lymphatics, and alveolar macrophages are shown in Figure 11. From 2 days to 2 wk there is a marked reduction in the number of fibers observed in all compartments. By 6 mo postexposure, fibers were no longer observed in the interstitium. By 12 mo, fibers were only observed either on the epithelial surface or in the lymphatics. Those fibers on the epithelial surface were not associated with macrophage or other cellular response (Figure 10, c, f).

While these confocal images provide quantification of where the chrysotile fibers are in the lung, they do not show the surrounding lung surfactant which is very important in mediating

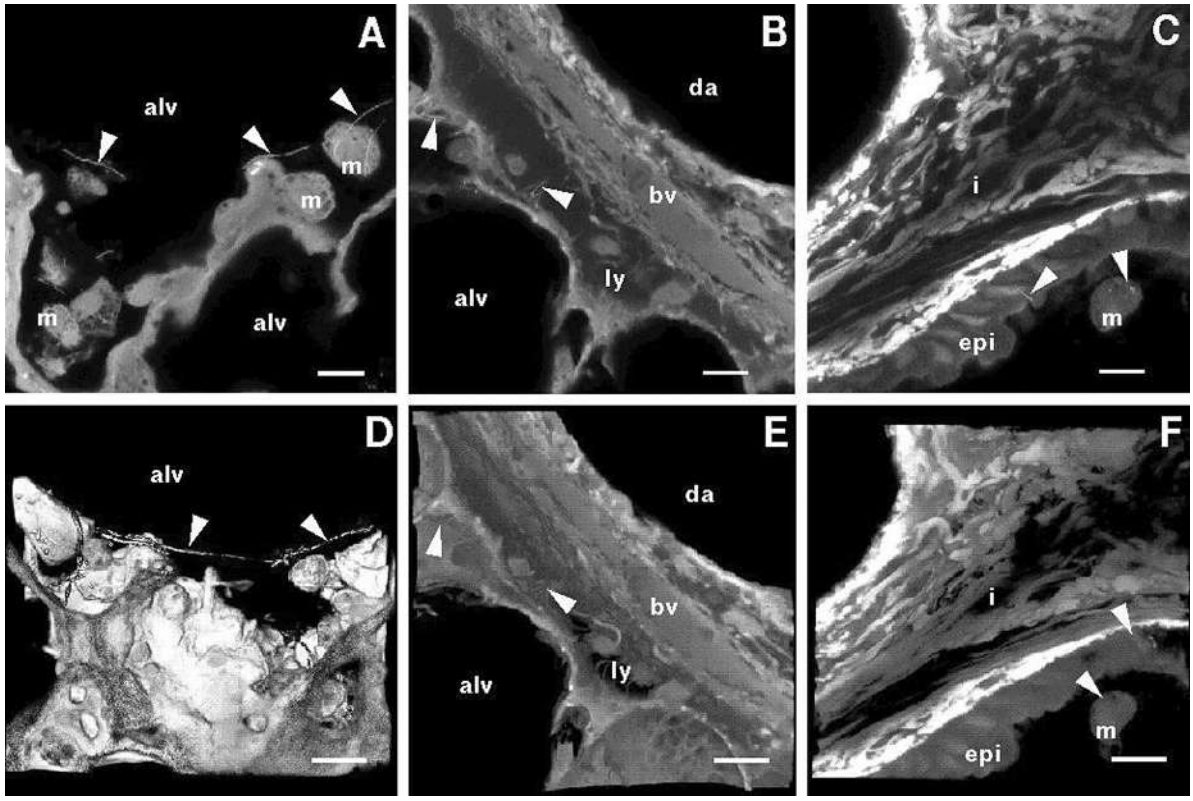

FIG. 8. Confocal micrographs of the lung at 2 days after cessation of exposure. (A), (B), (C) show an original single-scan image of the region. (D), (E), (F) show the reconstructed three-dimensional images of the same regions, which are composed of 70 serial sections. The length bars are 10 μm.

dissolution in the lung. Nearly all the fibers observed are within the surfactant layer and therefore more readily subject to dissolution with the biodegradation of chrysotile being diffusion-dependent (Atkinson, R. J., 1973). In addition, Etherington et al. (1981) has shown that macrophages can generate very low pH at the surface of the macrophage membrane and the attached particles, with pH values as low as 3.5 encountered. Chrysotile is most soluble at such acid pH. When in contact with dilute acids or even aqueous media at pH < 10, magnesium has been shown to readily dissociate from the fiber's surface (Atkinson, 1973; Hargreaves & Taylor, 1946; Nagy & Bates, 1952), resulting in a leached fiber (Atkinson, 1973). The results of our study are consistent with these proposed mechanisms leading to the breakup of longer chrysotile fibers into shorter pieces.

DISCUSSION

Fiber Structural Chemistry and Rapid Dissolution

In chrysotile, the magnesium hydroxide part of each layer is closest to the fiber surface and the silica tetrahedral is within the structure (see Figure 1). In water, the dissolution of chrysotile has been shown to be effected by the buffer capacity of the leach solution, with the amount of extractable Mg and SiO_2 increasing with increasing buffer strength (Smith, 1973). This reaction has been determined to be diffusion controlled through a layer of water near the mineral's surface.

In the lung, extensive work on modeling the dissolution of synthetic vitreous fibers (SVF) using in vitro dissolution techniques and inhalation biopersistence has shown that the lung has a very large buffer capacity (Mattson, 1994). These studies have shown that an equivalent in vitro flow rate of up to 1 ml/min is required to provide the same dissolution rate of SVF as that which occurs in the lung. In addition, chrysotile is more soluble at acid pH and thus may be affected by complete or even partial phagocytosis of fibers by macrophages.

With the chrysotile, it appears that as the magnesium dissolves that the fiber breaks apart into smaller pieces. Thus, while the rats were exposed to a very large number of long respirable fibers (450 fibers L > 20 μm/cm^3, GMD $= 0.096$ μm), that by day 6 of the study (1 day after cessation of exposure) already a large number of fibers had dissolved/broken apart.

Dose Delivered and Comparative Clearance

To assess how much of the deposited dose had been cleared from the lung by the first time point of analysis (day 1 after

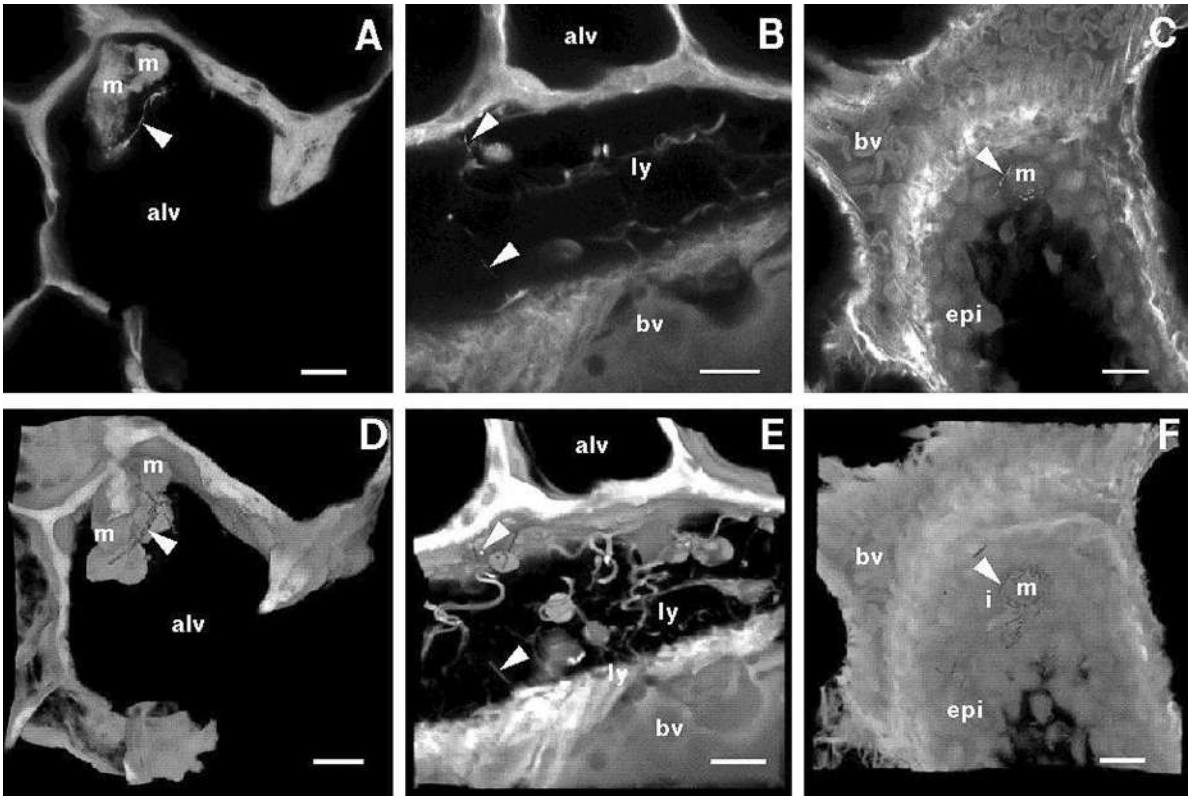

FIG. 9. Confocal micrographs of the lung at 2 wk after cessation of exposure. (A), (B), (C) show an original single-scan image of the region. (D), (E), (F) show the reconstructed three-dimensional images of the same regions, which are composed of 70 serial sections. The length bars are 10 μm.

cessation of exposure) and what the relative lung burdens are of chrysotile in comparison to amphibole asbestos and a highly soluble fiber, we compared the data from this study to the data from the two other biopersistence studies of chrysotile (Bernstein et al., 2003a, 2003b) as well as from a biopersistence study of tremolite asbestos, (Bernstein et al., 2003b), amosite asbestos, and the soluble stonewool fiber MMVF 34 (Hesterberg et al., 1998). In the amosite and MMVF 34 studies, the aerosol exposure concentrations were 150 fibers L $>$ 20 μm/cm^3. In the Canadian and Calidria chrysotile biopersistence studies the aerosol exposure concentrations were 200 fibers L $>$ 20 μm/cm^3. In the tremolite biopersistence study the aerosol exposure concentration was 100 fibers L $>$ 20 μm/cm^3. As described earlier, the chrysotile exposure concentrations were 450 fibers L $>$ 20 μm/cm^3.

With both amphiboles (amosite and tremolite), there is only a small amount of clearance of the long fibers following cessation of exposure, followed by virtually no further clearance. In the tremolite biopersistence study the histopathological response of the lungs was examined following the 5-day exposure and it was found that a granulomatous and fibrotic reaction was observed following cessation of exposure and persisted through the 12-mo observation period. In the same study, chrysotile showed no inflammatory or pathological response following the 5-day exposure (Bernstein et al., 2003b).

While all the chrysotiles cleared relatively quickly, differences were observed between the three types studied. The Calidria chrysotile, which is known to be a short fiber chrysotile, cleared the fastest, with a clearance half-time for the fibers longer than 20 μm of 0.3 days.

The clearance half-time of the Brazilian chrysotile was 1.3 days. At the end of 12 mo, 2 to 3 long fibers were measured following the lung digestion procedure. However, the exposure concentration for the Brazilian chrysotile was 465 fibers L $>$ 20 μm/cm^3, rather than the 150 to 200 fibers L $>$ 20 μm/cm^3 for the other fibers evaluated, thus resulting in a very high aerosol concentration of 2098 WHO fibers/cm^3 and 9226 total fibers/cm^3. It certainly is possible that this very high total exposure resulted in a response very different from what might be expected at lower exposure concentrations. Even so, the number of fibers observed at 12 mo was not statistically different than what was observed for the HT fiber, which had a 6-day clearance half-time for the long fibers. With the HT fiber neither fibrotic nor tumorigenic response was observed following a chronic inhalation toxicology study at similar numbers of long fibers (Kamstrup et al., 1998).

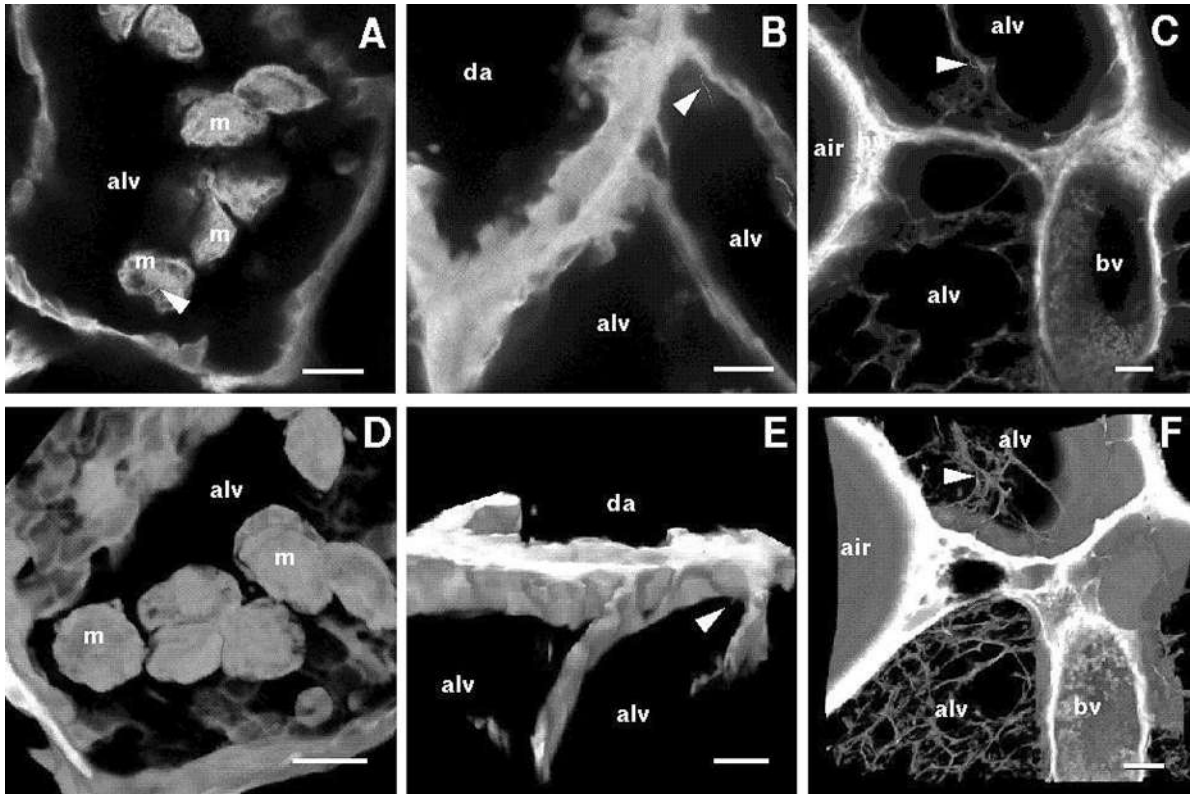

FIG. 10. Confocal micrographs of the lung at 6 mo (plates A–D and B–E) and at 12 mo (plates C and F) after cessation of exposure. (A), (B), (C) show an original single-scan image of the region. (D), (E), (F) show the reconstructed three-dimensional images of the same regions, which are composed of 70 serial sections. The length bars for (A), (B), (C), and (E) are 10 μm. For (C) and (F) the length bars are 50 μm.

The Canadian chrysotile studied was the long fiber textile grade and cleared with a clearance half-time of 11.4 days for the fibers longer than 20 μm (Bernstein et al., 2004). This number, however, is somewhat misleading as at 1 day after cessation of exposure, when the first measurement was made, there were already more than 50% fewer fibers remaining in comparison to the HT fiber or the amphiboles. This rapid reduction was observed even though the aerosol exposure concentration was 200 fibers L $>$ 20 μm/cm^3 for the Canadian chrysotile rather than the 150 fibers L $>$ 20 μm/cm^3 for the HT and amphiboles. This rate is illustrated in Figure 12, which shows the actual lung fiber measurements for each animal and in which the Canadian chrysotile and the HT fiber overlap in the period of 14 to 90 days. By 365 days there were no remaining long Canadian chrysotile fibers, even though, as mentioned earlier, a few HT long fibers remained.

Clearly there is a large difference in biopersistence between serpentine asbestos and amphiboles. In addition, as serpentine is a naturally occurring mined fiber, there appear to be some differences in biopersistence depending on where it is mined. However, chrysotile lies on the soluble end of this scale and ranges from the least biopersistent fiber to a fiber with biopersistence in the range of glass and stonewools. It remains less biopersistent than ceramic and special-purpose glasses (Hesterberg et al., 1998) and more than an order of magnitude less biopersistent than amphiboles.

Comparison With Other Chrysotile Biopersistence Studies

This study provides the third application of the EC biopersistence protocol to chrysotile. In the two studies reported earlier, Canadian chrysotile and Calidria (California) chrysotile have been evaluated (Bernstein et al., 2003a, 2003b). The clearance half-time for fibers longer than 20 μm was 11.4 days for the Canadian chrysotile and 0.3 days for the Calidria chrysotile. The clearance half-time for fibers longer than 20 μm for the Brazilian chrysotile in this study of 1.3 days again confirms that chrysotile is not biopersistent in the lung.

Ilgren and Chatfield (1998a) reviewed a number of previous studies that provided estimates of clearance of chrysotile based on the silica content of the lung. These studies reported clearance half-times considerably longer than that found here. This analysis, however, did not differentiate clearance as a function of fiber length or compartment within the lung. As seen in our

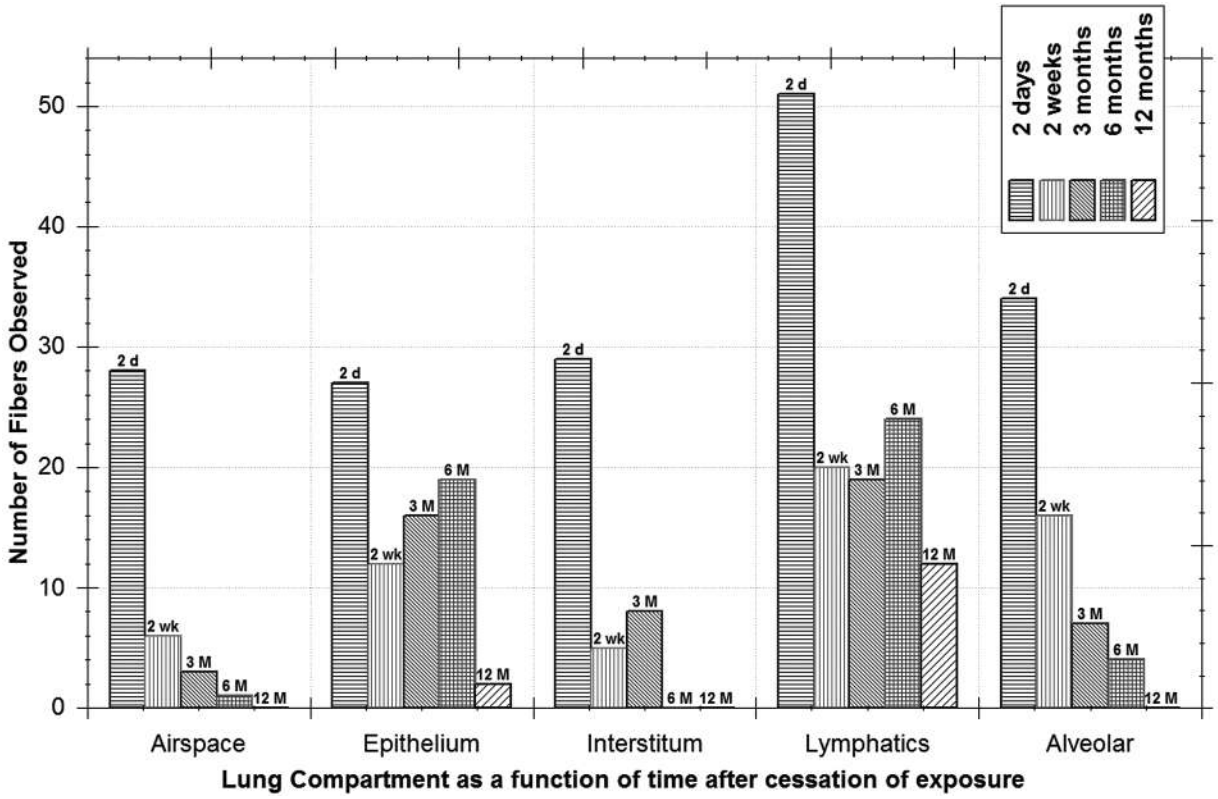

FIG. 11. Number of WHO fibers by lung compartment (confocal three-dimensional microscopic analysis).

study, the long chrysotile fibers clear most rapidly while some of the shorter fibers accumulate in the lung and lymphatics. Nearly all of these previous studies involved exposure periods of from 3 to 12 mo and used a range of exposure concentrations from 2 to 10 mg/m^3. Of particular importance in these studies is the lack on any investigation of concentration of other silicates present in the aerosol and especially of amphiboles fibers such as tremolite. Wagner et al. (1980) stated that "all materials contained impurities" in the chrysotile samples that they studied although they did not identify these impurities.

Short fiber clearance. For all fiber exposures, there are many more shorter fibers less than 20 μm in length and even more less than 5 μm in length. The clearance of the shorter fibers has in these studies been shown to be either similar to or faster than the clearance of insoluble nuisance dusts (Muhle et al., 1987; Stoeber et al., 1970).

The question of the possible effect of shorter chrysotile fibers has been addressed by the chronic inhalation studies reported by Ilgren and Chatfield (1997, 1998b). In these studies, exposure was 7 h/day, 5 days/wk for 12 mo to a mean concentration of 7.8 mg/m^3 of Coalinga chrysotile. The Coalinga chrysotile was reported as being relatively short, with the majority of fibers less than 5 μm in length. No fibrotic or tumorigenic response was observed following exposure to this fiber. Similar results were reported in another study with the Coalinga fiber by Muhle et al. (1987). In addition, the Coalinga fiber was tested in 4 chronic ip studies of up to 3 mg dose with tumor levels in the reported background range of up to 10% (Muhle et al., 1987; Pott et al., 1987; Rittinghausen et al., 1992). These studies provide support that shorter chrysotile is not carcinogenic following both inhalation and ip exposure at relatively high concentrations.

In another study, Davis et al. (1986) exposed groups of rats by inhalation to length classified amosite. The short fiber amosite (1.7% >5 μm in length) produced no malignant cancers in 42 rats, whereas the long-fiber amosite (30% >5 μm in length, 10% >10 μm), with the same diameter distribution, produced 8 cancers in 40 animals.

In a recent report issued by the Agency for Toxic Substances and Disease Registry entitled "Expert Panel on Health Effects of Asbestos and Synthetic Vitreous Fibers: The Influence of Fiber Length," the experts stated that "Given findings from epidemiologic studies, laboratory animal studies, and in vitro genotoxicity studies, combined with the lung's ability to clear short fibers, the panelists agreed that there is a strong weight of evidence that asbestos and SVFs (synthetic vitreous fibers) shorter than 5 μm are unlikely to cause cancer in humans" (ATSDR, 2003; U.S. EPA, 2003). In addition, Berman and Crump (2004) in their technical support document to the U.S. EPA on asbestos-related risk also found that shorter fibers do not appear to contribute to disease.

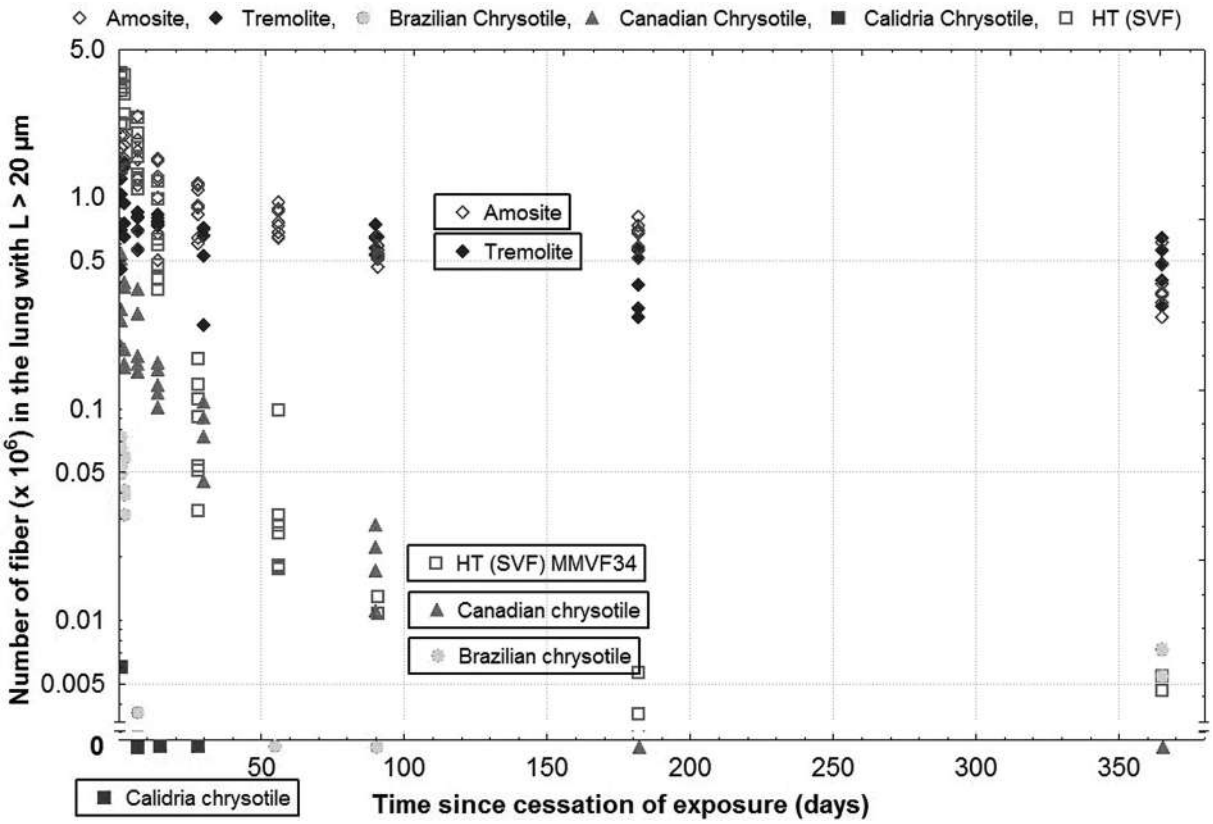

FIG. 12. Biopersistence of chrysotile, amphibole, and SVF: clearance of fibers with length greater than 20 μm.

Chronic inhalation studies. The biopersistence studies clearly differentiate between the serpentine chrysotile and the amphiboles, tremolite and amosite. These differences appear to be related to the differences in chemical structure between the serpentines and amphiboles and possibly the influence of the acidic pH associated with the macrophage on the chrysotile fiber.

However, when the chronic inhalation studies that have been performed on chrysotile and amphiboles are examined, these differences are not always apparent.

In an analysis of many of the animal dose-response studies that have been performed on asbestos, Berman et al. (1995) concluded that:

- Short fibers (less than somewhere between 5 and 10 μm in length) do not appear to contribute to cancer risk.
- Beyond a fixed, minimum length, potency increases with increasing length, at least up to a length of 20 μm (and possibly up to a length of as much as 40 μm).
- The majority of fibers that contribute to cancer risk are thin with diameters less than 0.5 μm and the most potent fibers may be even thinner. In fact, it appears that the fibers that are most potent are substantially thinner than the upper limit defined by respirability.
- Identifiable components (fibers and bundles) of complex structures (clusters and matrices) that exhibit the requisite size range may contribute to overall cancer risk because such structures likely disaggregate in the lung. Therefore, such structures should be individually enumerated when analyzing to determine the concentration of asbestos.
- For asbestos analyses to adequately represent biological activity, samples need to be prepared by a direct-transfer procedure.
- Based on animal dose-response studies alone, fiber type (i.e., fiber mineralogy) appears to impart only a modest effect on cancer risk (at least among the various asbestos types).

Concerning the lack of differentiation seen in the dose-response studies, the authors stated that this may be due at least in part to the limited lifetime of the rat relative to the biodurability of the asbestos fiber types evaluated in these studies. However, it should be noted as well that at the mass dose of 10 mg/m^3 used in most chrysotile chronic inhalation studies, the corresponding exposure concentration was approximately 1,000,000 particles and fibers/cm^3, 90% of which were particles

or short fibers. High concentrations of insoluble nuisance dusts have been shown to compromise the clearance mechanisms of the lung, causing inflammation and a tumorigenic response in the rat, a phenomenon often referred to as lung overload (Bolton et al., 1983; Muhle et al., 1987; Morrow, 1988; Oberdorster, 1995; Bellmann et al., 2003).

Summary

The mineralogy of the serpentine chrysotile fibers and amphiboles fibers shows distinct differences in the structure and chemistry of these two minerals. In contrast to the curled layered construction of chrysotile which appears to result in greater susceptibility to degradation, the amphibole fibers are rigid impermeable structures that are resistant to degradation. These differences are reflected in the inhalation biopersistence studies, which clearly differentiate chrysotile from the amphiboles and show that longer chrysotile fibers are rapidly eliminated from the lung while the longer amphiboles once deposited remain. Due to the difficulties in study design and the high particle/fiber exposure concentrations used, the chronic inhalation studies with asbestos are difficult to interpret, due in part to the nonspecific effects of such high particle concentrations used in these studies.

Recent quantitative reviews that analyzed the data of available epidemiological studies to determine potency of asbestos for causing lung cancer and mesothelioma in relation to fiber type also differentiated between chrysotile and amphibole asbestos (Hodgson and & Darnton, 2000; Berman & Crump, 2004). The most recent analyses also concluded that it is the longer, thinner fibers that have the greatest potency.

Brazilian chrysotile was found to be rapidly removed from the lung. Fibers longer than 20 μm were cleared with a half-time of 1.3 days, most likely by dissolution and breakage into shorter fibers. Shorter fibers were also rapidly cleared from the lung, with fibers 5–20 μm clearing even faster ($T_{1/2} = 2.4$ days) than those $<5\mu$m in length. The remaining short fibers were never found clumped together but appeared as separate, fine fibrils, occasionally unwound at one end. Short free fibers appeared in the corners of alveolar septa, and fibers or their fragments were found within alveolar macrophages. The same was true of fibers in lymphatics, as they appeared free or within phagocytic lymphocytes. These results further support the evidence that the chrysotile fibers are rapidly cleared from the lung, in marked contrast to amphibole fibers, which persist.

REFERENCES

Atkinson, R. J. 1973. Chrysotile asbestos: Colloidal silica surfaces in acidified suspensions. *J. Colloid Interface Sci*. 42:624–628.

Agency for Toxic Substances and Disease Registry. 2003. *Report on the Expert Panel on Health Effects of Asbestos and Synthetic Vitreous Fibers: The Influence of fiber length*. Atlanta, GA: Prepared for Agency for Toxic Substances and Disease Registry, Division of Health Assessment and Consultation.

Bellmann, B., Muhle, H., Creutzenberg, O., Ernst, H., Muller, M., Bernstein, D. M., and Riego Sintes, J. M. 2003. Calibration study on subchronic inhalation toxicity of man-made vitreous fibers in rats. *Inhal. Toxicol*. 15(12):1147–1177.

Berman, D. W., Crump, K. S., Chatfield, E. J., Davis, J. M., and Jones, A. D. 1995. The sizes, shapes, and mineralogy of asbestos structures that induce lung tumors or mesothelioma in AF/HAN rats following inhalation. *Risk Anal*. 15(2):181–195.

Berman, D. W., and Crump, K. S. 2004. *Technical support document for a protocol to assess asbestos-related risk*. Washington, DC: Office of Solid Waste and Emergency Response, U.S. Environmental Protection Agency.

Bernstein, D. M., Chevalier, J., and Smith, P. 2003a. Comparison of Calidria chrysotile asbestos to pure tremolite: inhalation biopersistence and histopathology following short-term exposure. *Inhal. Toxicol*. 15(14):1387–1419.

Bernstein, D. M., Mast, R., Anderson, R., Hesterberg, T. W., Musselman, R., Kamstrup, O., and Hadley, J. 1994. An experimental approach to the evaluation of the biopersistence of respirable synthetic fibers and minerals. *Environ. Health Perspect*. 102(Suppl. 5):15–18.

Bernstein, D. M., Riego Sintes, J. M., Ersboell, B. K., and Kunert, J. 2001a. Biopersistence of synthetic mineral fibers as a predictor of chronic inhalation toxicity in rats. *Inhal. Toxicol*. 13(10):823–849.

Bernstein, D. M., Riego Sintes, J. M., Ersboell, B. K., and Kunert, J. 2001b. Biopersistence of synthetic mineral fibers as a predictor of chronic intraperitoneal injection tumor response in rats. *Inhal. Toxicol*. 13(10):851–875.

Bernstein, D. M., and Riego-Sintes, J. M. R. 1999. *Methods for the determination of the hazardous properties for human health of man made mineral fibers (MMMF)*. Vol. EUR 18748 EN, April. 93, http://ecb.ei.jrc.it/DOCUMENTS/Testing-Methods/mmmfweb.pdf. European Commission Joint Research Centre, Institute for Health and Consumer Protection, Unit, Toxicology and Chemical Substances, European Chemicals Bureau.

Bernstein, D. M., Rogers, R., and Smith, P. 2003b. The biopersistence of Canadian chrysotile asbestos following inhalation. *Inhal. Toxicol*. 15(13):1247–1274.

Bernstein, D. M., Rogers, R., and Smith P. 2004. The biopersistence of Canadian chrysotile asbestos following inhalation: Final results through 1 year after cessation of exposure. *Inhal. Toxicol.* In press.

Bolton, R. E., Vincent, J. H., Jones, A. D., Addison, J., and Beckett, S. T., 1983. An overload hypothesis for pulmonary clearance of UICC amosite fibres inhaled by rats. *Br. J. Ind. Med*. 40:264–272.

Brismar, H., Patwardhan, A., G. Jaremko, and Nyengaard, J. 1996. Thickness estimation of fluorescent sections using a CLSM. *J. Microsc*. 184(2):106–116.

Cannon, W. C., Blanton, E. F., and McDonald, K. E. 1983. The flow-past chamber: An improved nose-only exposure system for rodents. *Am. Ind. Hyg. Assoc. J*. 44(12):923–928.

Cossette, M., and Delvaux, P. 1979. Technical evaluation of chrysotile asbestos ore bodies. In *Short course in mineralogical techniques of asbestos determination*, ed. R. C. Ledoux. Mineralogical Association of Canada, Toronto, Canada, pp.79–109, May.

Cruxên Barros de Oliveira, M. 1989. *Mineralogical analysis chrysotile*, tech rep 36 889. CEP 01064-970 São Paulo, Brazil: IPT, Instituto de Pesquisas Tecnológicas.

Davis, J. M., Addison, J., Bolton, R. E., Donaldson, K., Jones, A. D., and Smith, T. 1986. The pathogenicity of long versus short fibre samples of amosite asbestos administered to rats by inhalation and intraperitoneal injection. *Br. J. Exp. Pathol*. 67(3):415–430.

EPA. 2003. Report on the Peer Consultation Workshop to discuss a proposed protocol to assess asbestos-related risk. Prepared for U.S. Environmental Protection Agency, Office of Solid Waste and Emergency Response, Washington, DC 20460, EPA Contract No, 68-C-98-148, Work Assignment 2003–05. Prepared by Eastern Research Group, Inc., 110 Hartwell Avenue, Lexington, MA 02421. Final Report May 30, 2003.

Etherington, D. J., Pugh, D., and Silver, I. A. 1981. Collagen degradation in an experimental inflammatory lesion: Studies on the role of the macrophage. *Acta Biol. Med. Ger.* 40(10–11):1625–1636.

Hargreaves, A., and Taylor, W. H. 1946. An x-ray examination of decomposition products of chrysotile (asbestos) and serpentine. *Mineral. Mag.* 27:204–216.

Hesterberg, T. W., Chase, G., Axten, C., Miller, W. C., Musselman, R. P., Kamstrup, O., Hadley, J., Morscheidt, C., Bernstein, D. M., and Thevenaz P. 1998. Biopersistence of synthetic vitreous fibers and amosite asbestos in the rat lung following inhalation. *Toxicol. Appl. Pharmacol.* 151(2):262–275.

Hodgson, A. A. 1979. Chemistry and physics of asbestos. In *Asbestos: Properties, applications and hazards*, eds. by L. M. Chissick and S. S. Chissick, pp. 80–81. New York: John Wiley & Sons.

Hodgson, J. T., and Darnton, A. 2000. The quantitative risks of mesothelioma and lung cancer in relation to asbestos exposure. *Ann. Occup. Hyg.* 44(8):565–601.

Ilgren, E, and Chatfield, E. 1997. Coalinga fibre—A short, amphibole-free chrysotile. Evidence for lack of fibrogenic activity. *Indoor Built Environ*. 6:264–276.

Ilgren, E., and Chatfield, E. 1998. Coalinga fibre—A short, amphibole-free chrysotile part 2: Evidence for lack of tumourigenic activity. *Indoor Built Environ*. 7:18–31.

Ilgren, E., and Chatfield, E. 1998b. Coalinga fibre: A short, amphibole-free chrysotile, part 3: Lack of biopersistence. *Indoor Built Environ*. 7:98–109.

Kamstrup, O., Davis, J. M., Ellehauge, A., and Guldberg, M. 1998. The biopersistence and pathogenicity of man-made vitreous fibres after short- and long-term inhalation. *Ann. Occup. Hyg*. 42(3):191–199.

Kiyohara, P. K. 1991. *Estudo da interface crisotila-cimento Portland em compósitos de fibro-cimento por métodos óptico-eletrônicos*., Tese de Doutorado, apres. São Paulo:EPUSP.

Mattson, St. M. 1994. Glass fibres in simulated lung fluid: Dissolution behavior and analytical requirements. *Ann. Occup. Hyg*. 38:857–877.

McDonald, J. C., and McDonald, A. D. 1997. Chrysotile, tremolite and carcinogenicity. *Ann. Occup. Hyg*. 41(6):699–705.

Morrow, P. E. 1988. Possible mechanisms to explain dust overloading of the lungs. *Fundam. Appl. Toxicol.* 10(3):369–384.

Muhle, H., Pott, F., Bellmann, B., Takenaka, S., and Ziem, U. 1987. Inhalation and injection experiments in rats to test the carcinogenicity of MMMF. *Ann. Occup. Hyg*. 31(4B):755–764.

Nagy, B., and Bates, T. F. 1952. Stability of chrysotile asbestos. *Am. Mineral*. 37:1055–1058.

Oberdorster, G. 1995. Lung particle overload: implications for occupational exposures to particles. *Regul. Toxicol. Pharmacol*. 21(1):123–135.

Pott, F., Ziem, U., Reiffer, F. J., Huth, F., Ernst, H., and Mohr, U. 1987. Carcinogenicity studies on fibres, metal compounds, and some other dusts in rats. *Exp. Pathol*. 32(3):129–152.

Raabe, O. G., Yeh, H. C., Newton, G. J., Phalen, R. F., and Velasquez, D. J. 1977. Deposition of inhaled monodisperse aerosols in small rodents. In *Inhaled particles* IV, ed. W. H. Walton, Proceedings of an international symposium organized by the British Occupational Hygiene Society, Edinburgh, 22–26 September 1975, vol. 1, pp. 3–21. Oxford: Pergamon Press.

Rittinghausen, S., Ernst, H., Muhle, H., and Mohr, U. 1992. Atypical malignant mesotheliomas with osseous and cartilaginous differentiation after intraperitoneal injection of various types of mineral fibres in rats. *Exp. Toxicol. Pathol.* 44 (1):55–58.

Rogers, R. A., Antonini, J. M., Brismar, H., Lai, J., Hesterberg, T. W., Oldmixon, E. H., Thevenaz, P., and Brain, J. D. 1999. In situ microscopic analysis of asbestos and synthetic vitreous fibers retained in hamster lungs following inhalation. *Environ. Health Perspect.* 107(5):367–375.

Skinner, H. C. W., Ross, M., and Frondel, C. eds. 1988. *Asbestos and Other Fibrous* minerals. Oxford University Press.

Smith, R. W. 1973. Aqueous Surface Chemistry of Asbestos Minerals. National Inst. for Occupational Safety and Health, Cincinnati, OH. (Code: HEWOSH), Report number: PHS-OH-00332, NTIs Number: PB90-100942INZ. April.

Speil, S., and Leineweber, J. P. 1969. Asbestos minerals in modern technology. *Environ. Research* 2:166–208.

Stoeber, W., Flachsbart, H., and Hochrainer, D. 1970. Der Aerodynamische Durchmesser von Latexaggregaten und Asbestfassern. *Staub-Reinh. Luft.* 30:277–285.

Wagner, J. C., Berry, G., Skidmore, J. W., and Pooley, F. D. 1980. The comparative effects of three chrysotiles by injection and inhalation in rats. *IARC Sci. Publ* 30:363–372.

Weibel, E. R. 1984. *The pathway for oxygen.* Cambridge, MA: Harvard University Press.

World Health Organization 1985. *Reference methods for measuring airborne man-made mineral fibres (MMMF), WHO/EURO MMMF reference scheme*, Ed. WHO EURO Technical Committee for Monitoring and Evaluating Airborne MMMF, Vol. EH-4. Copenhagen: WHO.